

Hydro-morphological simulation of the stilling basin of Mazar dam with 3D schemes

Santiago Aurelio Ochoa-García ^a & Cristian Coello-Granda ^b

^a Unidad Académica de Ingeniería, Industria y Construcción, Universidad Católica de Cuenca, Cuenca, Ecuador. santiago.ochoa@ucacue.edu.ec

^b Ingestudios S.A.S, Cuenca, Ecuador. cristian.coello@ingestudios.com

Received: December 16th, 2022. Received in revised form: June 2nd, 2023. Accepted: June 7th, 2023.

Abstract

In the development of water resources projects with large hydraulic infrastructures, alterations to the natural flow regime will increase the erosive processes on the discharge structures due to variability of the turbulent velocities and the particle transport. We analyzed the case of the Mazar dam, a project designed to regulate the solid and liquid flows that come from the Paute river basin. Erosive processes of great magnitude are generated in the stilling basin of Mazar dam, due to the intensity of turbulent velocities produced in extreme events. We applied the Delft3D numerical model to simulate the hydrodynamic and sediment transport conditions to evaluate the stability conditions of the Mazar dam stilling basin. With the results obtained, vulnerable zones have been identified in the stilling basin. We recommended mitigation measures with the installation of a geomembrane to reduce the erosive processes in the vulnerable zones.

Keywords: hydrodynamics; morpho-dynamics; stilling basin; erosion; sedimentation.

Simulación hidro-morfológica del cuenco amortiguador de la presa de Mazar con esquemas 3D

Resumen

En el desarrollo de proyectos de aprovechamiento hídrico con grandes infraestructuras hidráulicas, se producen alteraciones del régimen de flujo natural que aumentan los procesos erosivos sobre las estructuras de descarga debido a la variabilidad de las velocidades turbulentas y transporte de partículas. Se analiza el caso de la presa Mazar, proyecto diseñado para regular los caudales sólidos y líquidos que provienen de la cuenca del río Paute. En el cuenco amortiguador de la presa de Mazar se generan procesos erosivos de gran magnitud, debido a la intensidad de las velocidades turbulentas en eventos extremos. Se aplicó el modelo numérico Delft3D para simular las condiciones hidrodinámicas y transporte de sedimentos, evaluando la estabilidad del cuenco amortiguador de la presa Mazar. Con los resultados obtenidos, se identificaron zonas vulnerables en el cuenco amortiguador. Se recomendaron medidas de mitigación con la instalación de geomembrana para atenuar los procesos erosivos en las zonas vulnerables.

Palabras clave: hidrodinámica; morfodinámica; cuenco amortiguador; erosión; sedimentación.

1 Introduction

Large hydraulic structures have been built for the use of water resources. In these structures, hydro-morphological processes have probably been modified. Understanding the hydro-morphological is essential for sustainable water management and the correct operation of different hydraulic structures [1]. Engineering problems related to the area of fluid mechanics can be solved through the continuous development of Computational

Fluid Dynamics (CFD), these schemes can be taken for the solution of turbulent flows with sediment transport and morphological changes [2]. State-of-the-art computational fluid dynamics (CFD) models can solve the Navier–Stokes equations in three dimensions with the volume of fluid (VOF) methods for free surface flow computation considering sediment transport and morphodynamics changes in large hydraulic structures [3].

The main objective of this work has been to simulate the hydro-morphological conditions of the stilling basin of Mazar

How to cite: Ochoa-García, S.A. and Coello-Granda, C., Hydro-morphological simulation of the stilling basin of Mazar dam with 3D schemes. DYNA, 90(227), pp. 14-23, July - September, 2023.

dam to identify areas vulnerable to regressive erosion. We apply the Delft3D numerical model to simulate the discharge structures of the Mazar dam. Delft3D has been used to carry out scenario-specific simulations of various flows, allowing optimization and evaluation of various aspects of different hydraulic projects [4].

In recent years numerous investigations have been carried out applying 3D numerical models with the solution of the Navier Stokes equations to simulate the hydrodynamic characteristics of stilling basins of different typologies (e.g., Demeke et al. [3], Ragessi et al. [5], Amorim et al. [6], Wang et al. [7], Siuta [8], Babaali et al. [9], Zhou and Wang [10], Khadka et al. [11], Mohammed et al. [12], Pereira de Morais et al. [13], Lu et al. [14]). However, we highlight the importance of numerical hydro-morphological simulation in environments of a stilling basin of a large regulating dam located at the confluence between two steep rivers.

Typical transport phenomena at river confluences [15] will be increased by the velocity of the flow that occurs in the hydraulic jump of the Mazar dam spillway, with shear forces of great magnitude that will generate erosive processes and instability in the banks of the stilling basin.

1.1 Study area

The Mazar dam is located in the Paute river basin (Fig. 1), where around 30% of Ecuador's hydroelectric energy is generated with the Paute project. The steep relief is representative in the middle and lower area, followed by a mountainous relief in the upper area. The Paute river basin has an area of 5066 km². The altitudinal ranges vary between 500 and 4800 meters above sea level [16].

The Paute hydroelectric complex is located in the provinces of Azuay, Cañar, and Morona Santiago in the foothills of the Andes Mountain range of the Republic of Ecuador. The hydroelectric development takes the waters of the Paute river, which is located between heights 2163 meters above sea level and 525 meters above sea level. It has four hydroelectric plants arranged in a cascade-type system: Mazar (170 MW), Molino (1100 MW), Sopladora (487 MW), and Cardenillo (596 MW). Currently, the project has

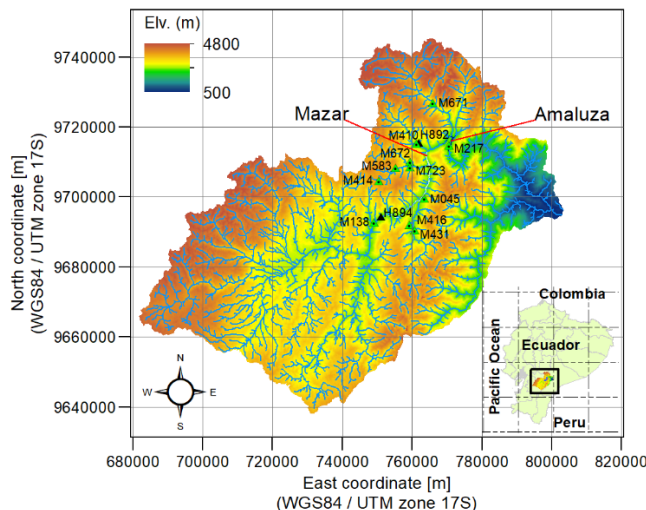


Figure 1. Paute river basin ubication.
Source: Own elaboration.

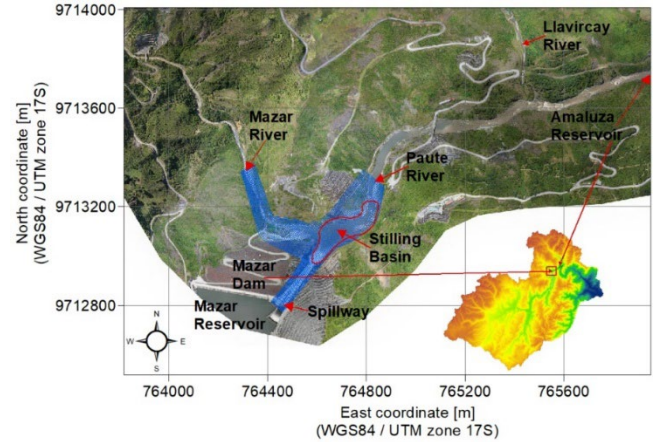


Figure 2. Mazar project ubication. Includes the numerical grid of the Delft3D model.

Source: Own elaboration.

three power plants (Mazar, Molino, and Sopladora) and two reservoirs (Mazar and Amaluza), while the Cardenillo power plant and the reservoir are the fourth and last stage of the complex, project that already has studies and designs definitive for its bidding and construction [17].

The Paute–Mazar hydroelectric plant is constituted the first element of the Paute Integral project. It is located just upstream of the union of the Paute river with the Mazar river (Fig. 2). The topography of the site is mountainous and irregular, with a mean annual temperature of 20 °C, relative humidity of 90%, and a mean annual rainfall of 2000 millimeters [18].

The main characteristic of the Mazar dam is the formation of a large reservoir (410 Hm³) that allows regulation of the flow of the Paute River, becoming the reserve for the hydro-energy production of the project. Additionally, the Mazar reservoir was designed to retain the solid materials transported from the upper and middle basins of the Paute river, allowing extend the useful life of the Amaluza reservoir (120 Hm³) for the operation of the Molino and Sopladora power plants [17].

The objective of a stilling basin is to reduce the kinetic energy of the discharge, to avoid the risk of undermining the basin and the structures located in the vicinity [12]. The energy dissipators are designed to withstand dynamic flow effects such as pulsations, vibrations, erosion, sedimentation, abrasion, and cavitation. However, eventually, any type of material will become vulnerable to the shear effects of flow [19].

According to the hydrological, hydraulic, and geometric characteristics of the Mazar dam stilling basin, the following particularities are sought to be simulated:

- Sediment transport from upstream of the Mazar river basin, most of which will be deposited immediately upstream of the stilling basin.
- Part of the material deposited upstream of the stilling basin will settle in the basin or downstream of it, transport processes that will be associated with both extreme flows and the restoration of the average flow in the Mazar river.
- In the events of flood flows in the Paute river, turbulent

velocities of great magnitude will be produced with three-dimensional fluctuations due to the discharge of the spillway and the ski jump. The magnitudes of the velocity on the stilling basin will generate zones of turbulent mixing, separation, and shear flow that will produce zones of local erosion, especially on the slope that is located just in front of the spillway. The magnitude of these processes will be increased when the floods in the Paute and Mazar rivers occur simultaneously.

The modeling domain covered an area of 19.84 Ha. The section considered includes the spillway of the Mazar dam and 528 meters stretch of the Mazar River until it reaches the confluence with the Paute River in the stilling basin. Fig. 2 displays the calculation mesh built for the simulation of the stilling basin and the following section details the considerations that have been made for the modeling in Delft3D.

2 Materials and methods

2.1 Initial Information

Adequate input data availability is the major challenge when developing hydro-morphological models [20]. The following data types were collected and processed before being used as input to the numerical model: bed topography, hydrometeorological data series, sediment transport, granulometry, and soil characteristics.

Different techniques were applied to obtain a suitable elevation model to represent the bed topography in the study domain. Initially, a drone flight was carried out to obtain the surface topographic survey using dual-frequency GNSS precision equipment, a Hasselblad camera, FPV goggles, and DJI Goggles. Additionally, it was necessary to apply three techniques to obtain the detail of the existing bathymetry and civil structures: 1) RTK Method, 2) Total Station Method, and 3) the Echosounder Method. The RTK system used corresponds to the TRIMBLE R10 equipment. The total station used was a TRIMBLE M3. The echo sounder used was the GARMIN GPSMap 722xs, which was linked to the GPS TRIMBLE R10.

Meteorological and discharges series considered were monitored by the Ecuadorian National Institute of Meteorology and Hydrology (INAMHI) and the Electric Corporation of Ecuador (CELEC) between 1964 and 2020. We considered eleven meteorological stations (M045, M138, M217, M410, M414, M416, M431, M583, M671, M672, M723 in Fig. 1), two hydrological stations (H892, H894 in Fig. 1) and the data series of the operation of Mazar dam. With the analysis of the hydrometeorological series and hydrological modeling with HEC-HMS, the hydrographs inflow boundaries (Fig. 3) that pass through the spillway and the Mazar River were obtained. The resulting hydrographs for return periods of 2, 5, 10, 25, 50, and 100 years are presented in Fig. 3.

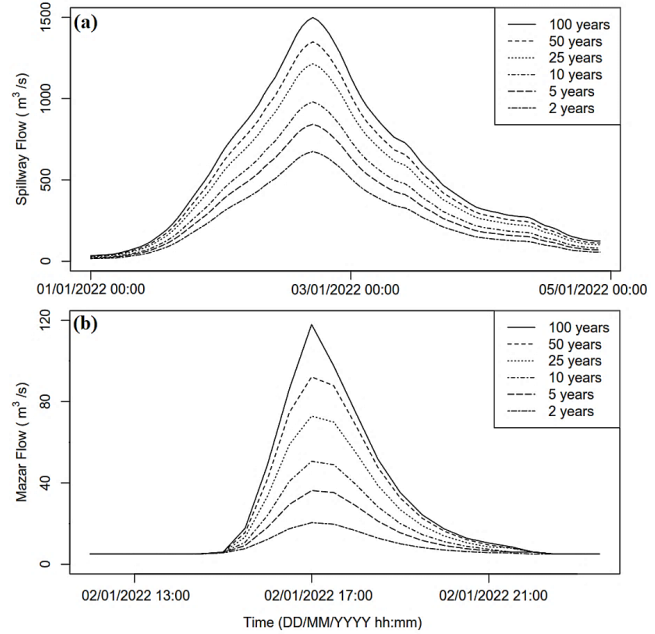


Figure 3. Spillway (a) and Mazar (b) river hydrographs. Source: Own elaboration.

For the choice of the maximum return period, it was taken into account that the structures of the stilling basin are complementary structures of the main spillway of the Mazar dam [21]. The peaks of the hydrographs presented in Fig. 3 had been made to coincide with the modeling, the maximum flow discharged on the stilling basin for the return period of 100 years corresponds to 1617 m³/s, of which 1499 m³/s corresponds to the flow of the Mazar reservoir that passes through the spillway and 118 m³/s to the flow of the Mazar river basin (16550 Ha).

To estimate the suspended sediment load coming from the Mazar River, samples taken by INAMHI and CELEC were analyzed. The entire processed series (38 points) shows an average mean concentration of 0.068 kg/m³ for flows between 5 m³/s to 16 m³/s. The hydro-morphological modeling considers flows with return periods greater than 2 years; we assumed a suspended solids load value of 0.1 kg/m³ from the Mazar River. Also, due to the considerable reduction in flow velocity in the Mazar reservoir [22], we neglected the suspended sediment load from the dam spillway.

To characterize the type of bed particles in the surroundings of the stilling basin, we analyzed the results of the soil analysis carried out by CELEC. The mean diameter (D_{50}) of the material has the order of 2 millimeters, the relative density in the order of 2.65, the dry density of the material in the order of 1600 kg/m³ and we assumed a porosity of 0.387 for the modeling.

To verify the results obtained in the modeling of the Mazar dam stilling basin with Delft3D, we used the results of the velocity variables documented in the reports of Ribas and Junji [23]. The physical model of the Mazar project was built with the likeness of Froude, at an undistorted scale of length 1:60, it is three-dimensional with a fixed bed. We presented in Fig. 4 the Physical model of the Mazar reservoir.



Figure 4. Physical Model of the Mazar Stilling Basin.
Source: Own elaboration.

Ribas and Junji [23] documented data of maximum velocity measured with a micro-current on the stilling basin for flows of 500 m³/s and 1350 m³/s, which corresponds to flows of 2 and 50 years of return period according to the considered hydrographs (Fig. 3(a)).

2.2 Numerical model

The model Delft3D used in this study solves the shallow-water equations 2D and 3D on the structured and unstructured grid, based on the finite-volume method. In 3D simulations, the vertical grid was defined following the sigma coordinate approach [24].

The hydrodynamic module (Delft3DFLOW) is based on the Reynolds-averaged Navier-Stokes (RANS) equations, which are simplified for an incompressible fluid under shallow water and Boussinesq assumptions. The RANS equations are solved by the alternative direction implicit finite difference method (ADI) on a spherical or orthogonal curvilinear grid [25]. Turbulence effects are computed employing the $K-\epsilon$ model. Horizontal background eddy viscosity and diffusivity are set equal to 1 m²/s [26].

The sediment transport and morphodynamics module (Delft3D-SED) considered both bedload and suspended load transport of non-cohesive sediments. The three-dimensional transport of suspended sediment is calculated by solving the

three-dimensional advection-diffusion (mass-balance) equation for the suspended sediment. We considered the sediment bed load transport formula of Van Rijn [27]. The change in the quantity of bed sediments caused by the bedload transport is calculated using the expression mass-balance in the bedload [24].

According to Stelling [28], a robust solver for shallow water equations has to satisfy the following demands: robustness, accuracy, suitability for both time-dependent and steady-state problems, and computational efficiency. The explicit time integration of the shallow water equations on a rectangular grid was subject to a time step condition based on the Courant number minor that one. The numerical grid generated to the Mazar still basin for Delft3D modeling (Fig. 2) consists of 13585 elements, whose size range varies from elements of approximately 2x2 meters in the densest part near the spillway to elements of approximately 10x10 meters in the least dense part of the mesh located in the vicinity of the stilling basin and considered that Courant restriction ($CFL < 1$). The number of vertical computational layers equals 10 with a high resolution near the bed (4% of the total height of the flow) decreasing towards the water surface (20% of the total height of the flow).

Four open boundaries were defined for the proposed modeling: two for inlet flow that Mazar dam spillways, one for inlet flow that Mazar River, and one outlet downstream. The inlet boundaries were defined with the hydrographs for the events considered (Fig. 3) and in the outlet boundaries, the water height was estimated for the different simulated flows considering Gradually Varied Flow and applying the Standard Step Method downstream of the Mazar still basin [29].

The boundary conditions that represent the flow resistance of solid boundaries were defined with the Manning friction coefficient (on the free surface, air resistance is neglected) [24]. Ibrahim and Abdel-Mageed [30] presented the importance of a correct choice of the Manning friction coefficient with flow results obtained in physical and numerical models with solid boundaries of different materials. The friction coefficient of the Delft3D model of the Mazar dam stilling basin has been defined according to the characteristics of the solid surface (Fig. 5(a)).

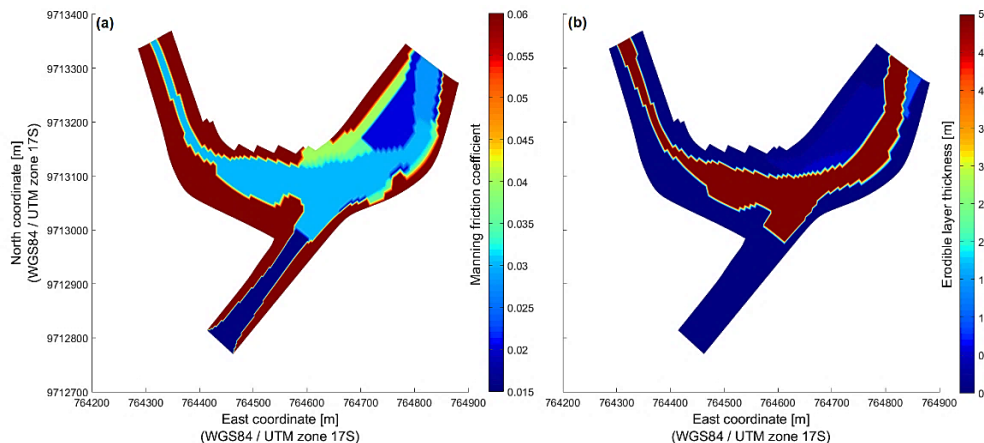


Figure 5. Manning Friction Coefficient (a) and Erodible Layer Thickness (b) definitions in the numerical model of the Mazar Stilling Basin.
Source: Own elaboration.

For the morphological updating, we defined a uniform bed layer with one sediment fraction according to the information available. The thickness definition of the total sediment layer in the spatial domain is non-uniformly distributed (Fig. 5(b)), considering zones in which bed erosion can be neglected (e.g., in the spillway) and zones with a great erodible thickness (e.g., in the river center bed). The spatial distribution of erodible thicknesses (Fig. 5(b)) was obtained from the exploration campaign with mechanical (direct exploration) and geophysical (indirect exploration) tests.

3 Results

3.1 Delft3D numerical results

To evaluate the model's performance, we considered the hydrodynamics results of the physical model of the Mazar project (Fig. 4) [23]. We considered statistical indices like the root-mean-square error (RMSE), the coefficient of determination (R^2), and percentage error (E%). The numerical model obtained that the simulated surface velocities were in the same order as the maximum velocities obtained in the physical model with a microcurrent device. Regarding statistical indices to evaluate the simulated results at the control points of the stilling basin, the RMSE obtained was 1.77 m/s, an R^2 of 0.83, and an average error of 22.95%.

We presented in Table 1 a summary of the statistical evaluation that contrasts the results of the velocity observed in the physical model of the Paute-Mazar hydroelectric and the velocity simulated with the Delft3D model.

The simulated velocities in DELFT3D were of the same order that the velocities observed in the physical model, but is evident that the numerical model would underestimate the

velocities concerning the physical model (Table 1). This could be explained because Ribas and Junji [23] reported the maximum velocities recorded with a microcurrent device, while the velocity results of the numerical model correspond to the average of the Navier Stokes equations. García y Niño [31] reported that the standard deviation of velocity fluctuations of a turbulent open channel flow is about 15% of the mean flow velocity. Also, to explain the differences in velocity results, continuous erosion produced from the beginning of the project should be considered. The change in the morphology of the discharge structures of the Mazar dam has modified the hydraulic conditions concerning the initial conditions considered for the configuration of the physical model. In Fig. 6 we presented the contour lines of the depth average velocity for the six return periods simulated with Delft3D.

Table 1.

Statistical evaluation of model performances for velocities.

ID-Point / Flow (m ³ /s)	North Coord. (m)	East Coord. (m)	Max. Velocity Obs. (m/s) ¹	Surface Velocity Sim. (m/s)	Percent. Error (%)
1a/500	764632.4	9713100.7	6.40	4.45	30.47
2a/500	764708.5	9713127.9	4.60	3.75	18.48
3a/500	764724.4	9713113.6	4.60	3.87	15.87
4a/500	764803.3	9713152.4	3.60	3.12	13.33
1b/1350	764639.6	9713109.8	8.40	6.95	17.26
2b/1350	764709.1	9713063	7.00	6.03	13.86
3b/1350	764751.9	9713084.4	7.00	4.73	32.43
4b/1350	764742	9713077.7	8.40	5.65	32.74
5b/1350	764835.6	9713232.4	8.40	5.7	32.14

Source: Own elaboration.

¹ Obtained from Ribas and Junji [23].

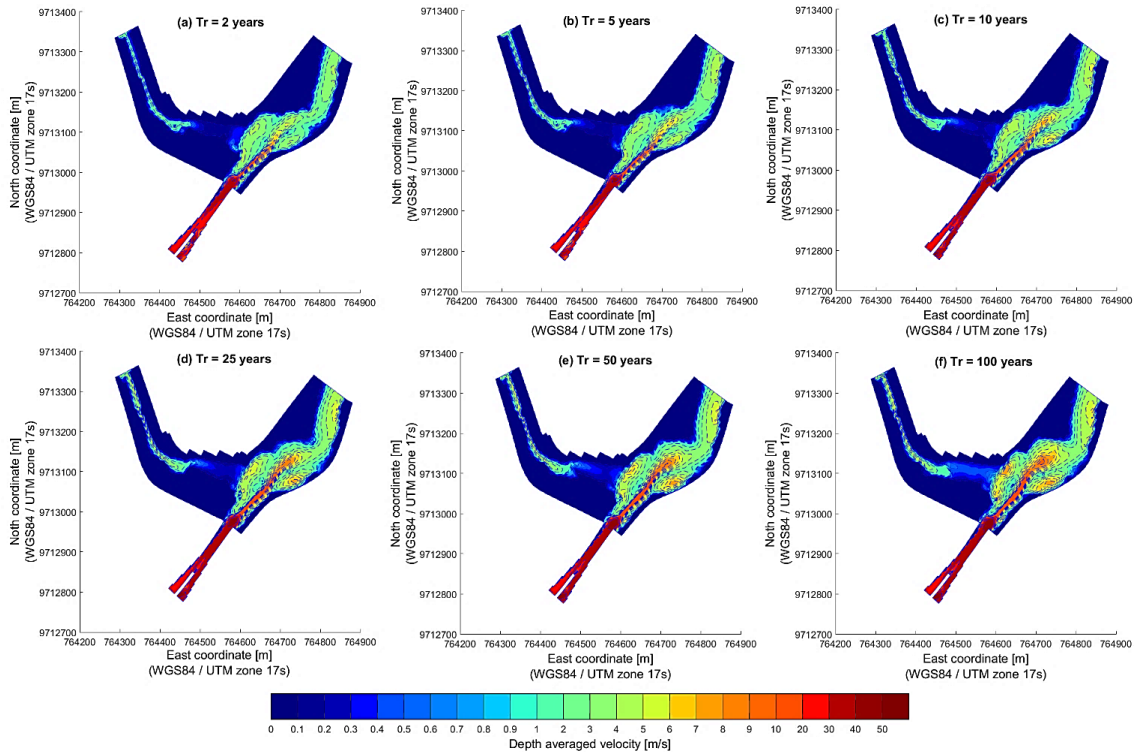


Figure 6. Depth average velocity in the Mazar stilling basin from return periods of 2 (a), 5 (b), 10 (c), 25 (d), 50 (e), and 100 (f) years.

Source: Own elaboration.

From the velocity results presented in Fig. 6, it is observed that the maximum flow velocities occur in the Mazar dam spillway with maximum magnitudes in the order of 50 m/s. Also, it is verified that the magnitude of the averaged velocities in the vertical increases according to the magnitude of the simulated events. In this sense, for the event with a return period of 100 years (Fig. 6(f)), at least three points susceptible to erosion were identified on the lateral slopes of the buffer basin with velocities greater than 8 m/s. The bed shear stress is a function of the flow velocity and water depth, therefore, to evaluate the vulnerable zones due to continuous erosion, we presented in Fig. 7 the results of water depth and the bed shear stress in the stilling basin for the peak event with a return period of 100 years.

In Fig. 7(a) was observed that the greatest flow depths occur in the center of the stilling basin with flow heights in the order of 20 meters, while in the spillway the flow heights are less than 2 meters for the return period of 100 years. In this sense, the magnitude of bed shear stresses in the spillway were one order of magnitude higher in contrast to the resulting bed shear stresses in the stilling basin, due to the low depth of the water and the high velocities that resulted in the spillway. In the zone of the Mazar river before discharge into the stilling basin, the bed shear stresses are of a lower magnitude in contrast to those resulting in the stilling basin. With the shear stress results in Fig. 7(b) three vulnerable zones could be identified near the slopes of the stilling basin, where the bed stresses were in the order of 700 N/m², magnitudes that produce continuous erosion on bed surfaces of natural channels [19].

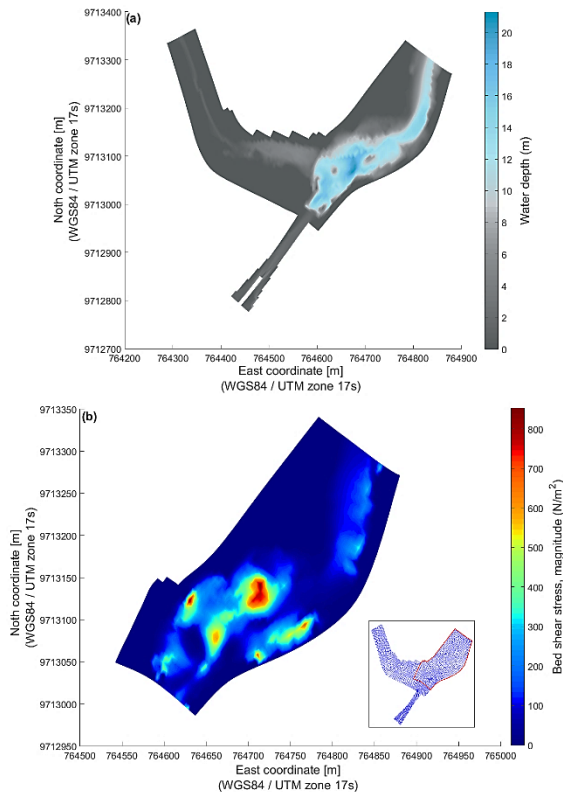


Figure 7. Water Depth (a) and Bed Shear Stress (b) simulating in the Mazar stilling basin from return period of 100 years. Source: Own elaboration.

With the application of sediment transport and morphodynamics computation module of Delft3D in the stilling basin of the Mazar dam, the bed changes for peak events were calculated in order to estimate erosion and deposition in the surroundings of the stilling basin. Fig. 8 shows the results of the initial and final bed morphology simulated in Delft3D for the return period of 100 years.

Fig. 8 shows erosion zones occurring mainly in the stilling basin, sedimentation zones are also observed on the Mazar river in the stretch immediately upstream of the confluence. With these results, it is possible to estimate the cumulative magnitude of erosion and sedimentation for the analyzed events (Fig. 9).

The results presented in Fig. 9 show that the eroded surface layer increases as events with return periods of greater magnitude were considered, with greater erosion in the center of the stilling basin and on its side slopes. However, sedimentation does not show a direct relationship with flow magnitude. Therefore, based on the results presented (Figs. 8 and 9) the erosion/sedimentation volumes corresponding to the analyzed events have been estimated (Table 2).

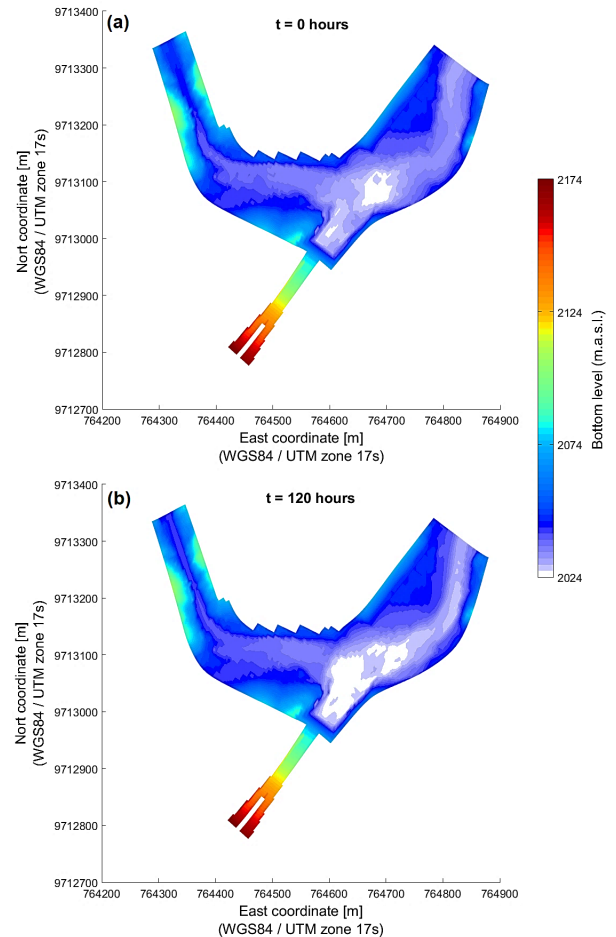


Figure 8. Initial Bed Morphology (a), Final Bed Morphology (b) and Cumulative Erosion/Sedimentation simulated in the Mazar stilling basin from return period of 100 years. Source: Own elaboration.

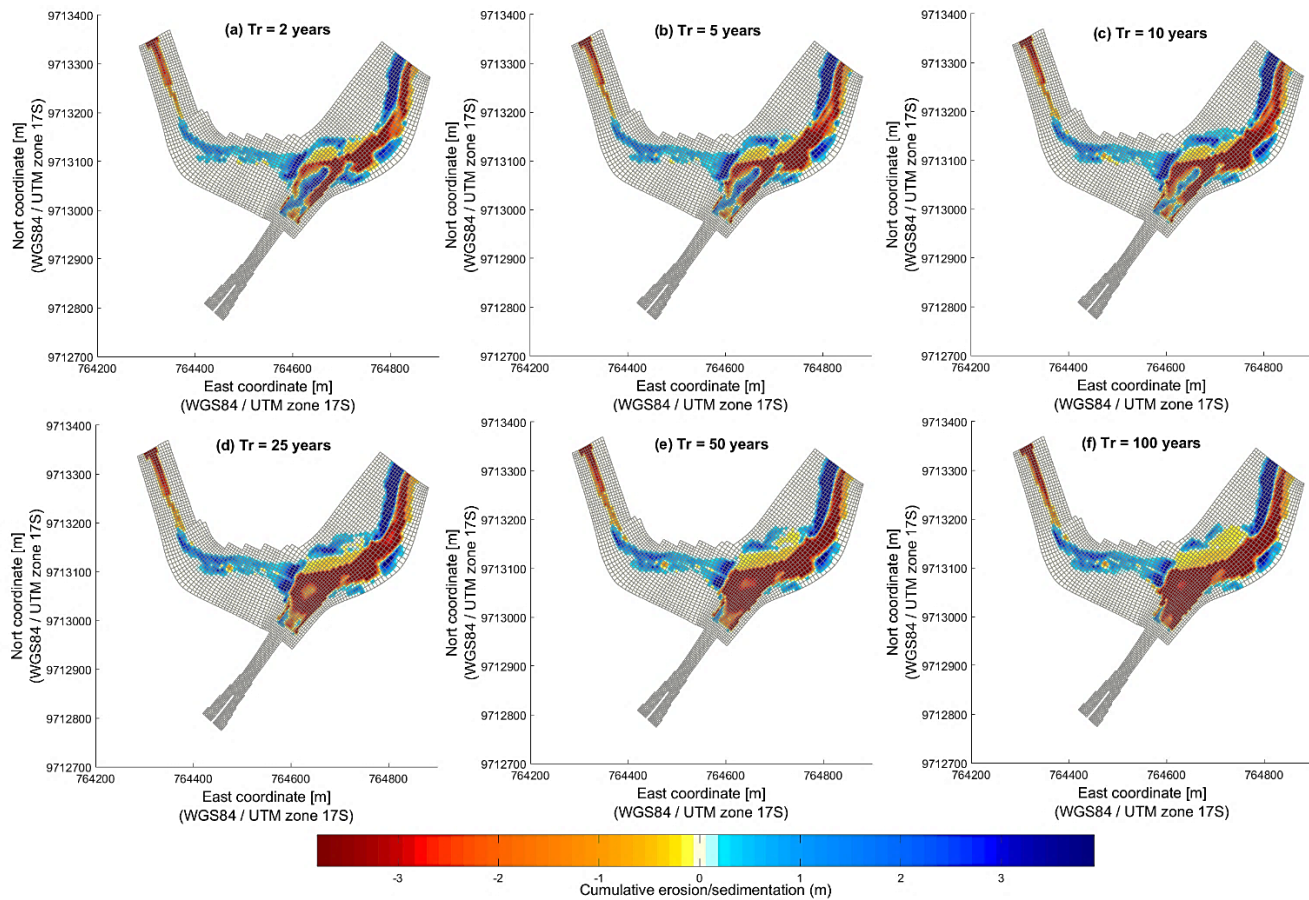


Figure 9. Cumulative erosion/sedimentation in the Mazar stilling basin from return periods of 2 (a), 5 (b), 10 (c), 25 (d), 50 (e), and 100 (f) years. Source: Own elaboration.

3.2 Protection measures on the banks of the stilling basin

In most cases, abrasion erosion damage in stilling basins has been the result of one or more of the following: a) construction diversion flows through constricted portions of the stilling basin; b) eddy currents created by diversion flows or powerhouse dis-charges adjacent to the basin; c) construction activities in the vicinity of the basin, particularly those involving cofferdams; d) no symmetrical discharges into the basin; e) separation of flow and eddy action within the basin sufficient to transport riprap from the exit channel into the basin; f) failure to clean basins after completion of construction work, and g) topography of the outflow channel [32].

The numerical simulation with Delft3D of the stilling basin of the Mazar dam shows the existence of an active lateral and bed erosion process due to the action of the flow in the Mazar dam structures, mainly due to the effect of the overflow of the excess spillway at the confluence of the Paute river with the Mazar river. Erosion occurs at specific points where the geology indicates the presence of colluvium, schist strata, and erodible phyllites.

According to the results of the hydrodynamic simulation with sediment transport, three sites have been identified with high vulnerability according to velocities,

shear stresses, and erosion levels. For the events considered, velocities in the order of 8 m/s were observed near the vulnerable sites on the slopes of the stilling basin (Fig. 6). According to these results, Fig. 10 shows the three sectors identified as vulnerable on the slopes of the stilling basin.

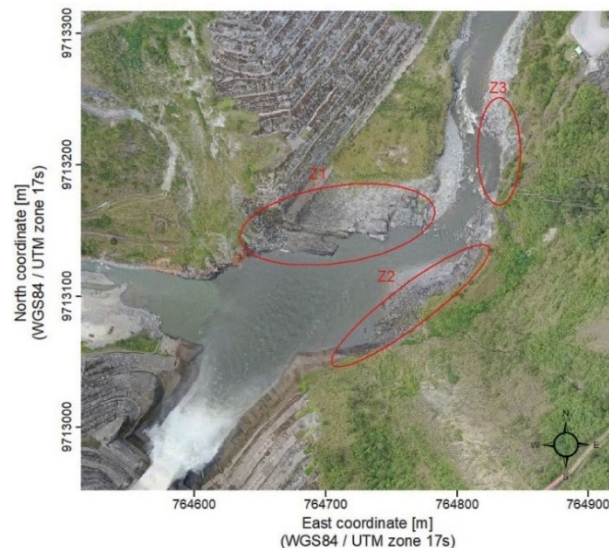


Figure 10. Vulnerable zones in the Mazar Dam stilling basin. Source: Own elaboration.


Zone 1 shown in Fig. 10 (Z1) presented the highest scour vulnerability, the discharge from the overflow weir strikes almost perpendicular to the slope, generating maximum flow velocities in the order of 12 m/s and bed shear stresses in the order of 1000 N/m². Z1 will be affected by the shear flow velocity of the Mazar river floods. Zone 2 (Z2) will be mainly affected by the discharge of the Mazar river in a perpendicular direction on this slope, generating maximum flow velocities in the order of 8 m/s and bed shear stresses in the order of 700 N/m². While the vulnerability of zone 3 (Z3) could be explained by the curvature at the outlet of the stilling basin that produces maximum velocities in the order of 5 m/s on the right slope, generating bed shear stresses in the order of 400 N/m².

There are several techniques now in use to stabilize an unstable slope. A few examples are bench terracing, fixing gabion walls, installation of masonry revetment walls, etc. However, in many cases, it has been experienced that slopes have failed to fail quickly if the soil surface is not covered with a suitable erosion control material [33].

In the case of the slopes of the Mazar dam's stilling basin, the main protective structures have been destroyed by the flow, this has occurred in the last ten years since the start of its operation in 2011. As a consequence, some stability has been achieved on the slopes, where weathered phyllite and shale material have been exposed. In order not to modify the morphological stability and to protect the surface from continuous erosion by the flow action of the spillway and Mazar River, the installation of a reinforced geomembrane (Table 3) we recommended in vulnerable areas to mitigate the erosive effects of turbulent flows and flood events.

An advantage of the double twisted mesh reinforced geomembrane is that it allows a firm fixing to the slope surface by the reinforcement mesh. It also allows the growth of foliage due to its 90% voids in its surface. The vegetation cover increases protection in areas of vulnerability to water flow erosion. The reinforced geomembrane has an estimated useful life of around 15 years and is less costly erosion protection than other reinforcement structures [34].

Table 3.
Geomembrane Characteristics.

Geomembrane reinforced with double twisted mesh ¹

Nominal thickness = 18 mm
Grammage ≥ 450 g/m ²
Predominant polymer = Polypropylene
Tensile strength = 34 kN/m
Elongation at break = 70%.
Maximum puncture force = 23.6 kN

¹ Source: MACCAFERRI [34].

4 Discussion

Numerical simulation of three-dimensional flow with changes in morphology identified areas vulnerable to continuous erosion in the buffer basin of the Mazar dam. The importance of the application of numerical simulation to verify the behavior of large hydraulic works is highlighted. However, even though the simulated flow variables tend to the real behavior, there are sources of error and uncertainty that must be analyzed looking for considerations that could improve the results of the numerical models implemented [35].

The main source of uncertainty in the models generated was due to the limited hydro-sedimentological information monitored over time [20]. To solve this situation, continuous monitoring of the Mazar and Paute rivers was recommended (installation of hydrometeorological stations, periodic bathymetries, liquid and solid gauging campaigns in control sections) in control sections in the vicinity of the Mazar dam's stilling basin, information that will serve as input data and for the calibration-validation of the generated models. The knowledge of the variability of the flow level and morphology for different events will allow us to have discharge curves for liquid and solid flows that will improve the contours and boundary conditions of the numerical models implemented.

Another issue of uncertainty is the spatial distribution of erodible thicknesses along the modeling domains [36]. The present study considered information obtained from the exploration campaign with mechanical (direct exploration) and geophysical (indirect exploration) tests. The direct tests consisted of two boreholes drilled with the roto percussion methodology and five exploration holes for the extraction of altered and unaltered samples. The geophysics consisted of two refraction seismic tests and one electrical tomography test [37]. In the refraction seismic tests, compressional wave velocity and shear wave velocity were measured, with this information, erodible thicknesses were estimated (Fig. 5(b)). We recommend periodic geological exploration studies to improve the characterization of the erodible layers that make up the riverbed and flood banks of the critical areas susceptible to instabilities.

Regarding the type of sediment simulated, the simulation considered uniform sediment of 2 millimeters according to the granulometric analysis of the material of the stilling pool. However, it is evident that the characterization of material varies spatially in the surroundings of the stilling basin, therefore, the uncertainty generated by this simplification could be reduced by considering a more detailed spatial distribution for the characteristics of the material in the erodible areas. In some areas cohesive soil may be considered in the simulation, all these considerations will have to be taken into account according to updated geological exploration studies [38]. With the efforts made to reduce the uncertainty of the model, it could be likely that there will be a variation in the simulated morphological changes, however, it should be expected that the vulnerability zones will be those already observed in the implemented model.

In the present work, extreme events with hydrographs of a 5-day duration were analyzed, which was considered adequate to evaluate the vulnerable zones in the surroundings of the Mazar dam's stilling basin. However, future research of interest would be to evaluate with numerical models the stability

conditions of the stilling basin considering protective geotextiles. For this scope, hydro-morphological models with long-term events could be considered.

5 Conclusions

Delft3D was applied for the hydrodynamic simulation of the flow with sediment transport and morphological evolution in the surroundings of the Mazar dam stilling basin, considering return periods of 2, 5, 10, 25, 50, and 100 years. The large-scale turbulent velocities with three-dimensional fluctuations generated by the discharge of high flows from the Mazar dam weir over the stilling basin formed zones of turbulent mixing, separation, and flow shear, identifying at least three zones vulnerable to continuous erosion.

With the results obtained, the three areas vulnerable to continuous erosion were evaluated according to the hydraulic and sediment transport conditions. The installation of reinforced geo-textiles in vulnerable areas was recommended to mitigate the erosive effects of turbulent flows in extreme events, taking into account the level of stability achieved after the alteration of structures and surface layers that has occurred since 2011.

It was observed that the sediment carried by the Mazar River will mostly be deposited immediately upstream of the stilling basin. Some of the material deposited upstream of the stilling basin will be accommodated in the basin or downstream of it. The central area of the stilling basin was identified as the area where the greater variability in morphology occurred for the events analyzed, which corresponds mostly to sediment transport downstream of the stilling basin.

References

- [1] Thanh, V.Q., Roelvink, D., van der Wegen, M., Reyns, J., Kernkamp, H., Vinh, G.V., and Linh, V.T.P., Flooding in the Mekong Delta: the impact of dyke systems on downstream hydrodynamics. *Hydrol. Earth Syst. Sci.*, 24, pp. 189-212, 2020. DOI: <https://doi.org/10.5194/hess-24-189-2020>.
- [2] Zeng, J., Constantinescu, G., and Weber, L., A 3D non-hydrostatic model to predict flow and sediment transport in loose-bed channel bends. *Journal of Hydraulic Research*, 46(3), pp. 356-372, 2008. DOI: <https://doi.org/10.3826/jhr.2008.3328>.
- [3] Demeke, G.K., Asfaw, D.H., and Shiferaw, Y.S., 3D Hydrodynamic modelling enhances the design of Tendaho Dam Spillway, Ethiopia. *Water*, 11, e82, 2019. DOI: <https://doi.org/10.3390/w11010082>.
- [4] Gyssels, P., Baldissoni, M., Hillman, G., Rodriguez, A., Bosc, J., Corral, M., Pagot, M., Brea, D., Spalletti, P. y Farias, H.D., Aplicaciones del modelo numérico DELFT3D a diferentes problemas hidrosedimentológicos en casos argentinos. *Asociación Argentina de Mecánica Computacional*, Vol XXXII, [en línea]. 2013, pp. 2757-2777, Disponible en: <https://cimec.org.ar/ojs/index.php/mc/article/view/4517>.
- [5] Ragessi, I.M., Damián, S.M., Guillén, N., Pozzi-Piacenza, C., García, C.M. y Hillman, G., Validación de un modelo numérico para la caracterización hidráulica de las obras de evacuación de la presa Los Molinos – Jujuy. *Asociación Argentina de Mecánica Computacional*, Vol XXXIII, [en línea]. 2014, pp. 337-347, Disponible en: <https://cimec.org.ar/ojs/index.php/mc/article/view/4644>.
- [6] Amorim, J.C.C., Amante R.C.R., and Barbosa V.D., Experimental and numerical modeling of flow in a stilling basin. E-proceedings of the 36th IAHR World Congress, [online]. 2015, The Hague, The Netherlands, Available at: <https://www.flow3d.com/wp-content/uploads/2014/04/Experimental-and-Numerical-Modeling-of-Flow-in-a-Stilling-Basin.pdf>.
- [7] Wang, Y., Wang, B., Zhang, H., Wang, Z., Zhou, S., and Ye, L., Three-dimensional numerical simulation on stilling basin of Sluice in low head. 5th International Conference on Civil, Architectural and Hydraulic Engineering, 2016, Zhuhai, China, DOI: <https://doi.org/10.2991/iccahe-16.2016.84>.
- [8] Siuta, T., The impact of deepening the stilling basin on the characteristics of hydraulic jump. *Environmental Engineering*, 115, pp. 173-186, 2018. DOI: <https://doi.org/10.4467/2353737XCT.18.046.8341>.
- [9] Babaali, H., Mojtahedi, A., Soori, N. and Soori, S., Numerical modeling of flow in USBR II stilling basin with end adverse slope. *International Journal of Environmental and Ecological Engineering*, 13(2), pp. 62-68, 2019. DOI: <https://doi.org/10.5281/zenodo.2571959>.
- [10] Zhou, Z., and Wang, J., Numerical modeling of 3D flow field among a compound stilling basin. *Mathematical Problems in Engineering*, 2019. DOI: <https://doi.org/10.1155/2019/5934274>.
- [11] Khadka, P., Bhattarai, S., Sharma-Ghimire, B.N., and Regmi, R.K., Numerical analysis of flow through stilling basin using CFD model. *International Journal of Civil Engineering and Technology*, 11(6), pp. 62-71, 2020. DOI: <https://doi.org/10.34218/IJCIET.11.6.2020.008>.
- [12] Mohammed, S.R., Nile, B.K., and Hassan, W.H., Modelling stilling basins for sewage networks. 3rd International Conference on Engineering Sciences, IOP Conf. Series: Materials Science and Engineering 671, 2020. DOI: <https://doi.org/10.1088/1757-899X/671/1/012111>.
- [13] Pereira de Moraes, V.H., Gireli, T.Z. and Vatauvuk, P., Numerical and experimental models applied to an ogee crest spillway and roller bucket stilling basin. *Brazilian Journal of Water Resources*, 25, e18, 2020. DOI: <https://doi.org/10.1590/2318-0331.252020190005>.
- [14] Lu, Y., Yin, J., Yang, Z., Wei, K., and Liu, Z., Numerical Study of fluctuating pressure on stilling basin slab with sudden lateral enlargement and bottom drop. *Water*, 13, e238, 2021. DOI: <https://doi.org/10.3390/w13020238>.
- [15] Rhoads, B.L. and Sukhodolov, A., Lateral momentum flux and the spatial evolution of flow within a confluence mixing interface. *Water Resources Research*, 44(8), e06634, 2008. DOI: <https://doi.org/10.1029/2007WR006634>.
- [16] Celleri, R., Willems, P., Buytaert, W. and Feyen, J., Space-time rainfall variability in the Paute Basin, Ecuadorian Andes. *Hydrological Processes*, 21(24), pp. 3316-3327, 2007. DOI: <https://doi.org/10.1002/hyp.6575>.
- [17] CELEC E.P., Unidad de Negocio CELECSUR. [en línea]. 2022. Disponible en: <https://www.celec.gob.ec/celec-sur/>.
- [18] Cedillo, A.P. and Jara, E.G., Modelación del ciclo de nutrientes en los embalses Mazar y Amaluza del proyecto hidroeléctrico Paute, Azuay. Tesis de grado, Facultad de Ingeniería, Universidad de Cuenca, Ecuador, [en línea]. 2015. Disponible en: <http://dspace.ucuenca.edu.ec/handle/123456789/21599>.
- [19] ACI Committee 210. Erosion of concrete in hydraulic structures (Reapproved 2008). *American Concrete Institute*, 1987, ACI 210R-93, 1-24, ISBN: 9780870314292.
- [20] Barrera, P.D., Mosselman, E., Giardino, A., Becker, A., Ottevanger, W., Nabi, M. and Arias-Hidalgo, M., Sediment budget analysis of the Guayas River using a process-based model. *Hydrol. Earth Syst. Sci.*, 23, pp. 2763-2778, 2019. DOI: <https://doi.org/10.5194/hess-23-2763-2019>.
- [21] Ponce, V.M., *Engineering Hydrology, Principles and Practices*. 2014, Second Edition, Online Version, <http://ponce.sdsu.edu/enghydro/index.html>.
- [22] Patil, R., and Shetkar, R., Prediction of sediment deposition in reservoir using analytical method. *American Journal of Civil Engineering*, 4(6), pp. 290-297, 2016. DOI: <https://doi.org/10.11648/j.ajce.20160406.14>.
- [23] Ribas, F., and Junji, J., Proyecto HL-144-estudios hidráulicos en modelo reducido del aprovechamiento hidroeléctrico de Pau-te-Mazar. Reports 01-05, Instituto de Tecnología para o Desenvolvimento, Centro de Hidráulica e Hidrologia Prof. Pa-rigot De Souza. 2007.
- [24] DELTARES. Simulation of multi-dimensional hydrodynamic flows and transport phenomena, including sediments. *Delft3D-Flow, User Manual*, [online]. 2022. Available at: https://content.oss.deltares.nl/delft3d/manuals/Delft3D-FLOW_User_Manual.pdf.

- [25] Zhang, L., Lu, J., Chen, X., Liang, D., Fu, X., Sauvage, S., and Sanchez-Perez, J.M., Stream flow simulation and verification in ungauged zones by coupling hydrological and hydrodynamic models: a case study of the Poyang Lake ungauged zone. *Hydrol. Earth Syst. Sci.*, 21, pp. 5847-5861, 2017. DOI: <https://doi.org/10.5194/hess-21-5847-2017>.
 - [26] Brière, C., Giardino, A., and van der Werf, J.J., Morphological modeling of bar dynamics with Delft3D: the quest for optimal free parameter settings using an automatic calibration technique. *Coastal Engineering Proceedings*, 1(32), sediment.60., 2010. DOI: <https://doi.org/10.9753/icce.v32.sediment.60>.
 - [27] Van Rijn, L.C., *Principles of sediment transport in rivers, estuaries and coastal seas*. Aqua Publications - 111, 1993, The Netherlands, ISBN: 9789080035690.
 - [28] Stelling, G., On the construction of computational methods for shallow water flow problems. PhD. Thesis, Rijkswaterstaat Communication Series No. 35, Rijkswaterstaat, The Hague, [online]. 1984. Available at: <http://resolver.tudelft.nl/uuid:d3b818cb-9f91-4369-a03e-d90c8c175a96>.
 - [29] Chow, V.T., *Open-Channel Hydraulics*. McGraw-Hill Book Company, Tokyo, Japan, 1959.
 - [30] Ibrahim, M.M., and Abdel-Mageed, N.B., Effect of bed roughness on flow characteristics. *International Journal of Academic Research*, 6(5), pp. 169-178, 2014. DOI: <https://doi.org/10.7813/2075-4124.2014/6-5/A.24>.
 - [31] García, M.H., and Niño, Y., *Flow and transport equations in surface waters*. Spring Sem, Department of Civil and Environmental Engineering, University of Illinois at Urbana-Champaign, CEE 498 Environmental Hydrodynamics, 2003.
 - [32] McDonald, J.E., Maintenance and preservation of concrete structures: report 2. U.S. Army Engineer Waterways Experiment Station, Technical Report No. C-78-4, Repair of Erosion Damaged Structures, Vicksburg, [online]. 1980. Available at: <https://erdc-library.erdc.dren.mil/jspui/handle/11681/2420>.
 - [33] Choudhury, P.K., Das, A., Goswami, D.N., and Sanyal, T. Bio-Engineering approach with Jute Geotextile for slope stabilization. *Proceedings of the 4th Asian Regional Conference on Geosynthetics*, Shanghai, China, 2008, pp. 863-864. DOI: https://doi.org/10.1007/978-3-540-69313-0_156.
 - [34] MACCAFERRI. MACMAT® R1 80 POLIMAC™ en malla hexagonal de doble torsión con polimac. Especificación Técnica, E-8.2.2-337-rev.01, [online]. 2018. Available at: <https://www.maccaferri.com/br/es/productos-lista/>.
 - [35] Viti, N., Valero, D. and Gualtieri, C., Numerical simulation of hydraulic jumps. Part 2: recent results and future outlook. *Water*, 11, art. 28, 2019. DOI: <https://doi.org/10.3390/w11010028>.
 - [36] Yin, D., Xue, Z.G., Gochis, D.J., Yu, W., Morales, M., and Rafieeiniasab, A., A process-based, fully distributed soil erosion and sediment transport model for WRF-Hydro. *Water*, 12, art. 1840, 2020. DOI: <https://doi.org/10.3390/w12061840>.
 - [37] Carollo, A., Patrizia, C., and Martorana, R., Joint interpretation of seismic refraction tomography and electrical resistivity tomography by cluster analysis to detect buried cavities. *Journal of Applied Geophysics*, 178, art. 104069, 2020. DOI: <https://doi.org/10.1016/j.jappgeo.2020.104069>.
 - [38] Zhao, Y., Liu, L., Kang, S., Ao, Y., Han, L., and Ma, C., Quantitative analysis of factors influencing spatial distribution of soil erosion based on geo-detector model under diverse geomorphological types. *Land* 10, art. 604. 2021. DOI: <https://doi.org/10.3390/land10060604>.
- S.A. Ochoa-García**, is BSc. Eng in Civil Engineer in 2009, from the “Universidad de Cuenca” (UCUE), Ecuador. Sp. in Hydraulics in 2013, MSc. with mention in Water Resources in 2014, and PhD in Engineering Sciences in 2018, all of them from the Universidad Nacional de Córdoba (UNC), Argentina. From 2013 to 2018, he was a research fellow in the Hydraulics Department of the Faculty of Exact, Physical and Natural Sciences (FCEPyN-UNC). From 2018 to 2020, he worked as specialist in hydrology at “Corporación de Energía Eléctrica del Ecuador” (CELEC E.P.). Currently, he is a full-time professor and researcher of the Civil Engineering career at the Universidad Católica de Cuenca (UCACUE), Ecuador. His research interests include: hydraulics, hydrology, computational fluid dynamics and geographic information systems applied to water resources.
ORCID: 0000-0001-9695-5976
- C. Coello-Granda**, is BSc. Eng in Civil Engineer in 2003, from the University of Cuenca (UCUE), Ecuador. MSc. in Soil and Water Management and Conservation in 2005, from the University of Cuenca, Ecuador in alliance with the Catholic University of Leuven and Gent of Belgium. He carried out his activities as a researcher and consultant in the Water and Soil Management Program (PROMAS) of the University of Cuenca (2006-2019). He was a professor in the Faculty of Civil Engineering at the University of Cuenca in the period 2012 - 2016 teaching subjects related to water resources. He is currently founder and Director of INGESTUDIOS Consulting Company since 2021. He has written several scientific articles related to watershed hydrology, meteorology and river hydraulics.
ORCID: 0009-0007-7181-4684